Spatiotemporal variations of stress and strain in the crust near 2019 Ridgecrest Earthquake Sequence

Niloufar Abolfathian[1], Eric J. Fielding[1]

[1]Jet Propulsion Laboratory, California Institute of Technology

We analyze 2 years postseismic deformation of the 2019 Mw 7.1 Ridgecrest earthquake sequence employing both seismic and geodetic data including InSAR and GPS. We use geodetic data to measure the postseismic surface deformation, and infer the associated afterslip, in addition to image pre-earthquake deformation. The interferograms are obtained from ARIA (Caltech-JPL Advanced Rapid Imaging and Analysis) products, which has been systematically processing InSAR data from the Copernicus Sentinel-1 satellites. Two tracks of C-band SAR data cover the study area, recording more than 30 interferograms from each of the ascending track 64 and the descending track 71 every 6 and 12 days. GPS data are obtained from GeoGateway, which is a data product and analysis tool developed by NASA consisting of geodetic imaging products. The estimated postseismic deformation is consistent with the main right-lateral NW-SE rupture. The largest surface uplift and the largest displacement in the afterslip model are located near the Mw 7.1 hypocenter. We also examine the associated stress field inverting more than 4,500 fault plane solutions within the same postseismic time period and estimate the 4D spatiotemporal stress field variations in the study area. Overall, the stress field estimations indicate higher extensional stress components in the NW of the main rupture shifting to higher compressional components in the SE adjacent to the Garlock fault. The spatiotemporal stress field evolution during the postseismic period shows the largest variations in the upper 4 km of the crust, indicating the heterogeneous brittle region and the least variations deeper than 8 km indicating higher viscoelastic component near the brittle-ductile transition zone. Integrating the obtained afterslip, strain-rate and stress field, we investigate locations with higher variations in the strain-rate and stress field to detect zones that are potential for higher stress accumulations and seismic hazard.

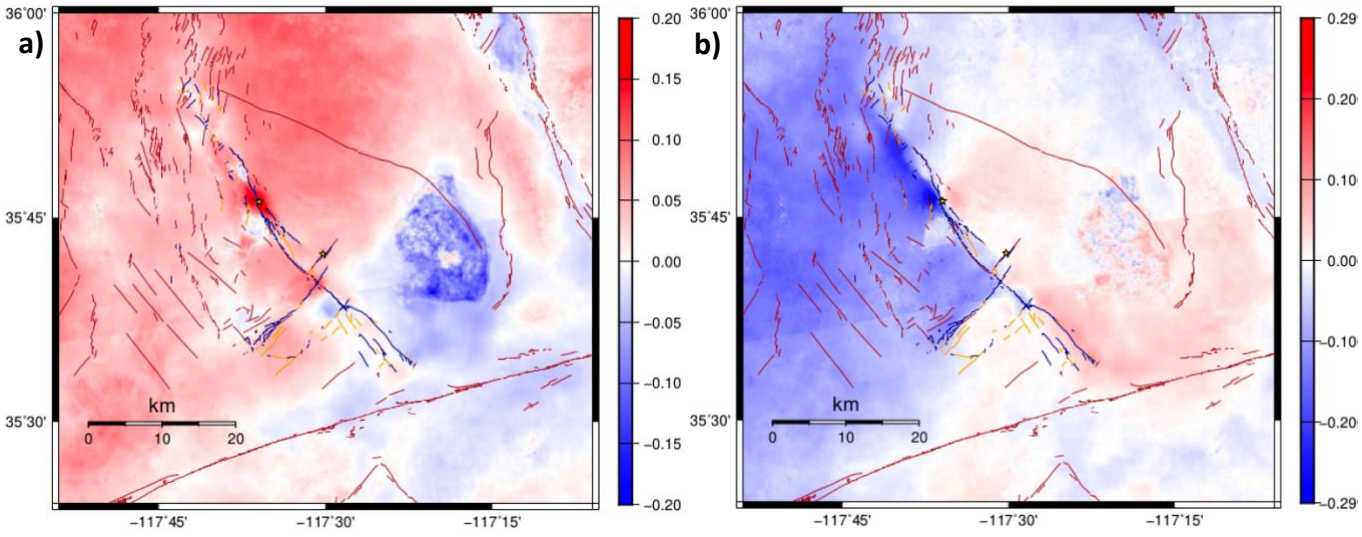

Figure. a) Vertical velocity (m/yr) and **b)** Horizontal velocity towards east (m/yr) from combination of tracks A64 and D71.